Journal of Molecular Catalysis A: Chemical 316 (2010) 112–117

Contents lists available at ScienceDirect

Journal of Molecular Catalysis A: Chemical

journal homepage: www.elsevier.com/locate/molcata

A revisit to proline-catalyzed aldol reaction: Interactions with acetone and catalytic mechanisms

Gang Yang[a,b,*], Zhiwei Yang[b], Lijun Zhou[b], Rongxiu Zhu[a], Chengbu Liu[a,**]

[a] Institute of Theoretical Chemistry, Shandong University, Jinan 250100, PR China
[b] Key Laboratory of Forest Plant Ecology, Ministry of Education, Northeast Forestry University, Harbin 150040, PR China

ARTICLE INFO

Article history:
Received 15 June 2009
Received in revised form 1 October 2009
Accepted 6 October 2009
Available online 13 October 2009

Keywords:
Density functional calculations
Proline
Aldol reaction
Enamine formation
Organocatalysis

ABSTRACT

In this work, density functional calculations were employed to revisit the formation mechanism of enamine, the intermediate to mediate the proline-catalyzed direct aldol reaction. Different from the work of Boyd et al. [24], the plausible reaction routes were calculated on basis of the complete conformational studies of proline and acetone interacted complexes. Six energy minima were determined and their relative stabilities increase in the order **PAf** < **PAe** < **PAb** < **PAc** < **PAa** < **Pad**. These structures are mainly stabilized through the hydrogen bonds of the proline-H atoms and the acetone-O atoms. Routes 2 and 4 are the most probable to take place. The rate-determining step of Route 2 is the formation of C3–N bond with the energy barrier equal to 86 kJ mol^{-1}. This step is accelerated by the following barrierless process. As the theoretical results indicated, Route 4 needs to start with at least 2 mole equiv. acetone, consistent with the high acetone concentrations used in experiments. The rate-determining step of Route 4 is the intra-carboxyl proton transfer, which was revealed to be greatly assisted by solvents.

1. Introduction

The aldol reaction establishes itself in organic synthesis owing to the facile formation of C–C bonds. Recently, List, Sakthivel and their co-workers [1–3] have demonstrated that the amino acid proline is an effective asymmetric catalyst for the direct aldol reaction. These pioneering studies brought the revival of modern organocatalysis. To date, various proline-based organocatalysts have been designed for the direct aldol reaction and compared with proline, some of them exhibit superior catalytic efficiency and enantioselectivity [4–8].

Theoretical calculations play an important role in the understanding of reaction mechanisms and designing of organocatalysts [4,9–19]. It was assumed that the aldol reaction proceeds via an enamine-mediated mechanism [1,2,20–23]. The stereoselectivities of proline-catalyzed asymmetric aldol reactions were predicted by density functional calculations at B3LYP/6-31G(d) level, achieving reasonable agreement with the experimental data [10]. As the theoretical calculations of Wu et al. [4] indicated, the energy barriers of the L-prolinamide catalyzed aldol reactions are greatly reduced by the hydrogen bonds of the amide N-H and terminal O-H groups with the benzaldehyde substrates. However, all these calculations [4,9–16] focused on the latter portions of the catalytic processes, with the enamine intermediates having already formed. It is also of high values to understand how to form the enamine intermediates. To the best of our knowledge, only one report from Boyd's group [24] is available in this aspect, see Scheme 1. Firstly, the **1a** structure is formed from the proline and acetone interactions. Step 1 (**1a** → **1c**) is the proton transfer from the amino group to the carbonyl group. Step 2 (**1c** → **1e**) forms the imine structure bound with a water molecule, which is then released. Step 3 (**1f** → **1h**) is the conformational transition towards the enamine intermediate. At B3LYP/6-311+G(2df,p)//B3LYP/6-31G(d,p) level, Step 1 has a large energy barrier of 171 kJ mol^{-1} and hinders the further progression. In our opinion, the aldol reaction needs a revisit mainly due to the two reasons: (1) only one interacting mode of proline and acetone (**1a** in Scheme 1) was given [24]. We cannot make sure whether it is the global energy minimum or the only structure to initiate the reaction. (2) The transition state of Step 1 contains a four-membered ring and is known to be geometrically unstable. In this work, a conformational analysis on the proline and acetone interacted system was performed. According to the previous theoretical calculations [25–29], four conformers of proline have notable populations at moderate temperatures. Two in Scheme 2 were chosen for this study, including the one of Boyd et al. [24]. The other two differ from them in the puckering angle of the pyrrolidine ring not involved in the aldol reaction; in addition, their energies are very close to the two of this study [27–29]. On such basis, all the plausible reaction routes were taken into calculations, aiming to find out the ones with rational transition states and

* Corresponding author at: Institute of Theoretical Chemistry, Shandong University, Jinan 250100, PR China. Tel.: +86 451 82192223; fax: +86 451 82102082.
** Corresponding author. Fax: +86 451 82102082.
E-mail address: theobiochem@gmail.com (G. Yang).

1381-1169/$ – see front matter © 2009 Elsevier B.V. All rights reserved.
doi:10.1016/j.molcata.2009.10.008

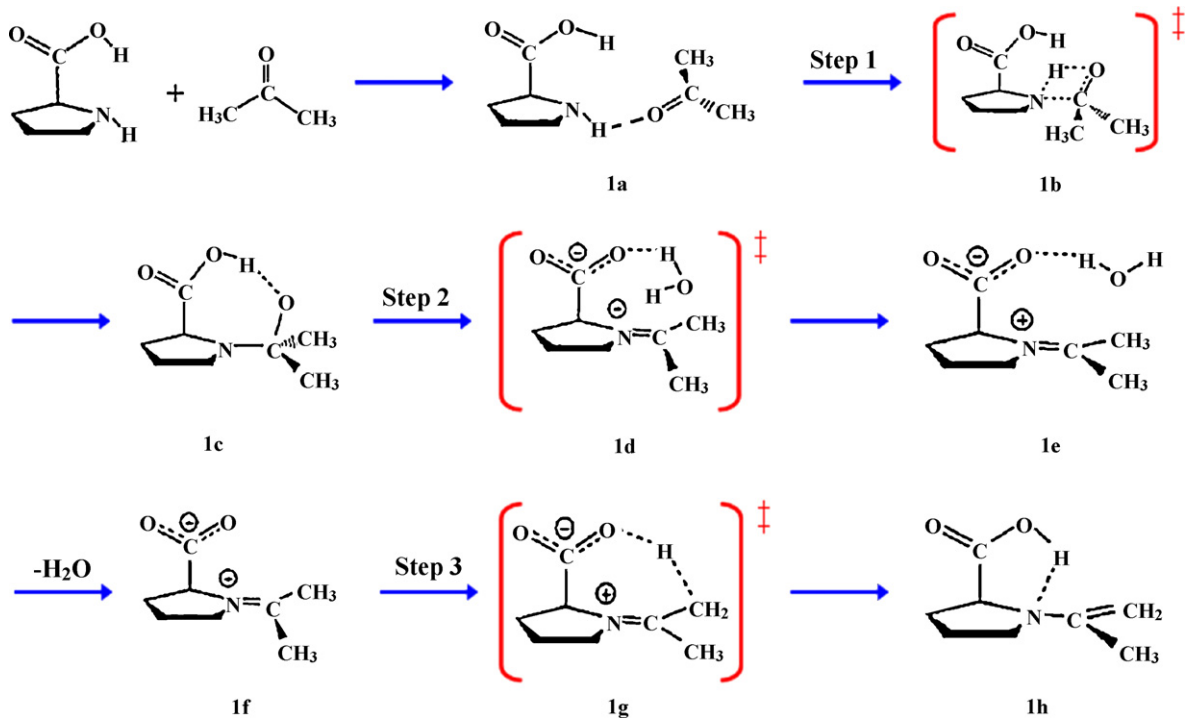

Scheme 1. The catalytic reaction route of the enamine formation proposed by Boyd et al. [24]. The nominations of the structures (**1a**–**1h**) follow the work of Boyd et al., and those within the square brackets represent transition states (TS). The reaction route is divided into three steps and labeled as Steps 1–3.

low energy barriers as well as aiding the understanding towards the proline-based organocatalytic processes.

2. Computational details

All the calculations were performed within Gaussian03 suite of programs [30]. The structures were optimized using B3LYP density functional [31,32], which combines Becke's three-parameter hybrid exchange functional (B3) and Lee, Yang, and Parr correlation functional (LYP). In agreement with Ref. [24], the standard 6-31G(d,p) basis set was used for geometry optimizations. Frequency calculations at the same level were performed, making sure that the local energy minima and transition states have none and one imaginary vibration, respectively. The solvent effects were considered by the self-consistent isodensity polarizable continuum model (SCI-PCM) of self-consistent reaction field (SCRF) [33] as previously used [34–36]. The default dielectric constant of 46.7 was adopted for DMSO.

Also in agreement with Ref. [24] in order to make comparisons, all the energy calculations were run at B3LYP/6-311+G(2df,p) level of theory, using the B3LYP/6-31G(d,p) optimized geometries, which were then corrected with appropriate zero-point vibrational energies (ZPVE), i.e., B3LYP/6-311+G(2df,p)//B3LYP/6-31G(d,p)+ZPVE.

3. Results and discussion

3.1. Proline and acetone interacted structures

Six energy minima were determined for the proline and acetone interacted system, see Fig. 1. **PAa**, **PAb** and **PAc** originate from the first proline isomer (**Pro1** in Scheme 2a). The three structures are of close energies with the differences not more than 2 kJ mol^{-1}. In all the structures, the proline amino-H2 atoms form hydrogen bonds with the acetone carbonyl-O3 atoms, and the three hydrogen bonds are of close distances, ranging within 2.069–2.285 Å. **PAb** resembles the structure used in Ref. [24] (i.e., **1a** in Scheme 1) and is slightly more unstable than **PAa** and **PAc**. The main geometric discrepancy between **PAa** and **PAb** is the orientation of the acetone methyl group. In **PAa**, only the methyl-H3 atom has medium interactions with the carboxyl-O1 atom, and the H4 atom is directed

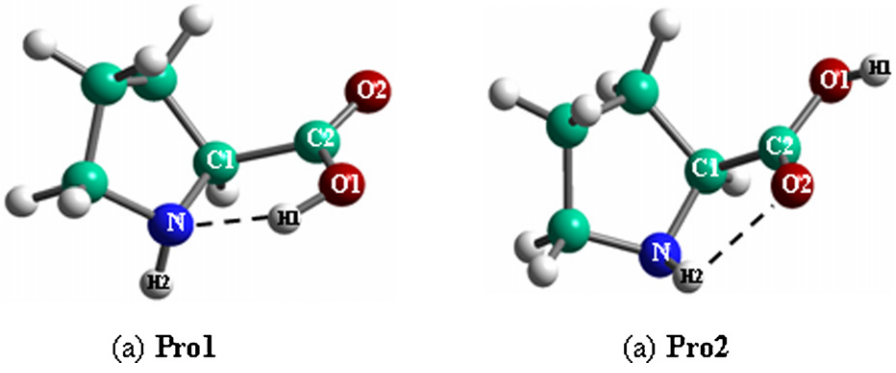

Scheme 2. Two proline isomers chosen for the present studies.

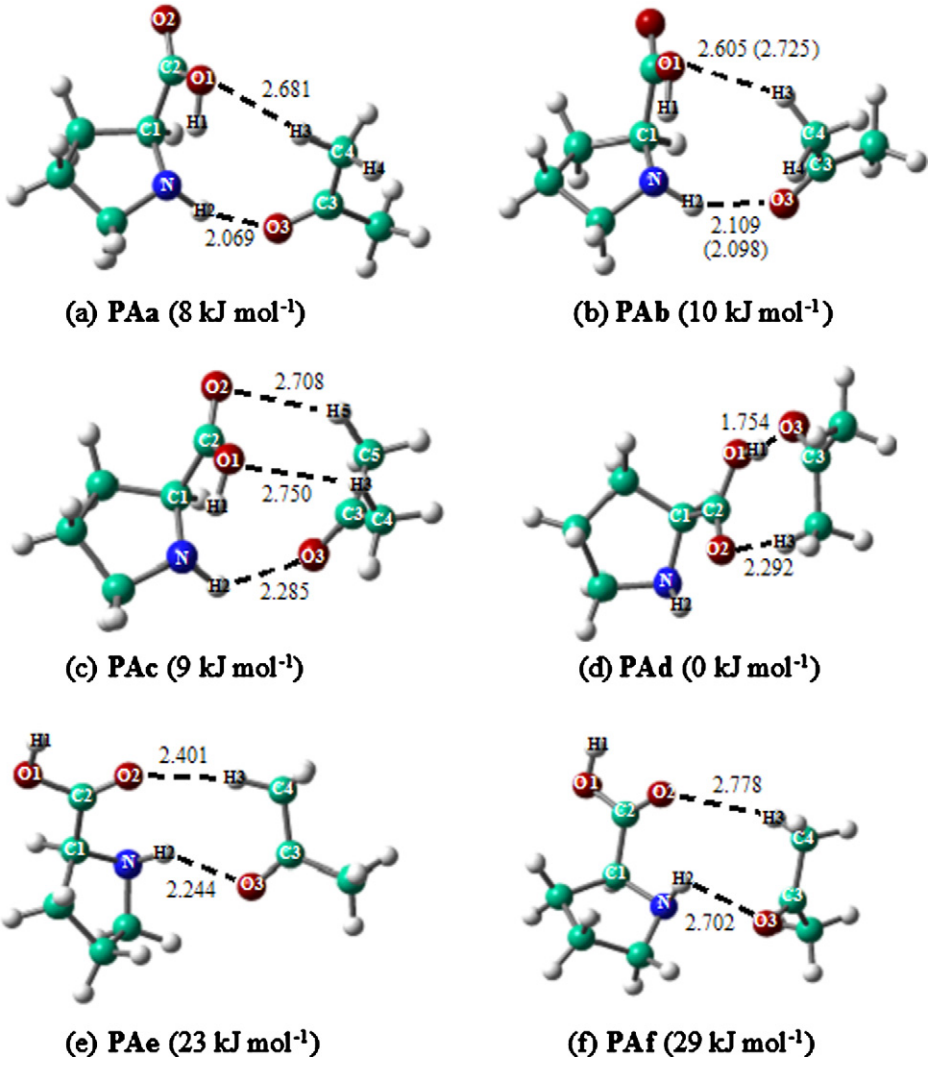

Fig. 1. (a)–(f) Structures and relative energies of proline and acetone interacting system. The distances of the proline and acetone interacting structure used in Ref. [24] (**1a** in Scheme 1) were given in the parentheses of **PAb**.

opposite to the O1 atom with a large O1–H4 distance of 4.301 Å. However, both H3 and H4 atoms in **PAb** are at the same side of the carboxyl group, and the H3–O1 and H4–O1 distances were optimized at 2.605 (2.725) and 3.675 (3.601) Å, respectively. The values in parentheses were taken from the **1a** structure [24]. Different from **PAa** and **PAb**, both of the methyl groups in **PAc** interact with the carboxyl-O atoms with the O1–H3 and O2–H5 distances of 2.750 and 2.708 Å, respectively.

The interactions of acetone with the other proline isomer (**Pro2** in Scheme 2b) can also form three energy minima, seeing **PAd**, **PAe** and **PAf** in Fig. 1. **PAd** is much more stable than **PAe** and **PAf** and the energy gaps were calculated to be larger than 22 kJ mol^{-1}. **PAd** is the global minimum on the potential energy surface (PES), and its superior stability may be due to the presence of the carboxyl-H1 → carbonyl-O3 hydrogen bond. Instead, the acetone-O3 atoms in the other five structures form hydrogen bonding interactions with the amino-H2 atoms. Analogous to **PAa** and **PAb**, one methyl-H atom of acetone in **PAe** and **PAf** has medium interactions with the carboxyl-O atom and the H4–O2 distances equal 2.401 and 2.778 Å, respectively.

3.2. Catalytic reaction routes starting from ***Pro1***

As discussed above, the interactions of **Pro1** with acetone produce the **PAa**, **PAb** and **PAc** structures and among them, **PAa** is of

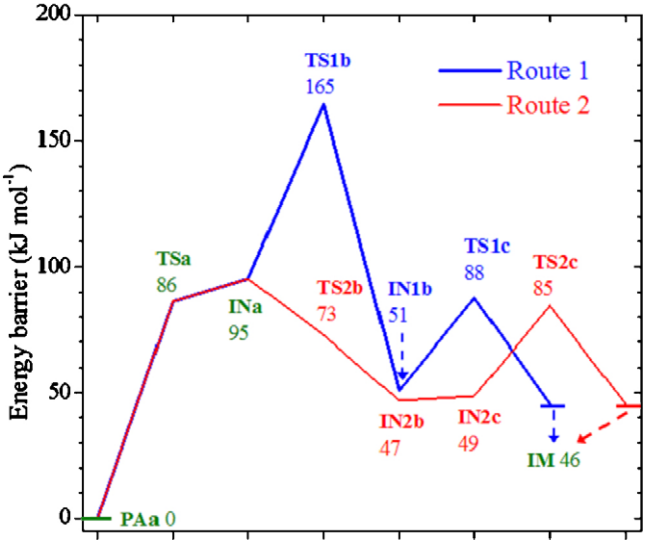

Fig. 2. Energy profiles of the imine formation starting from **PAa**.

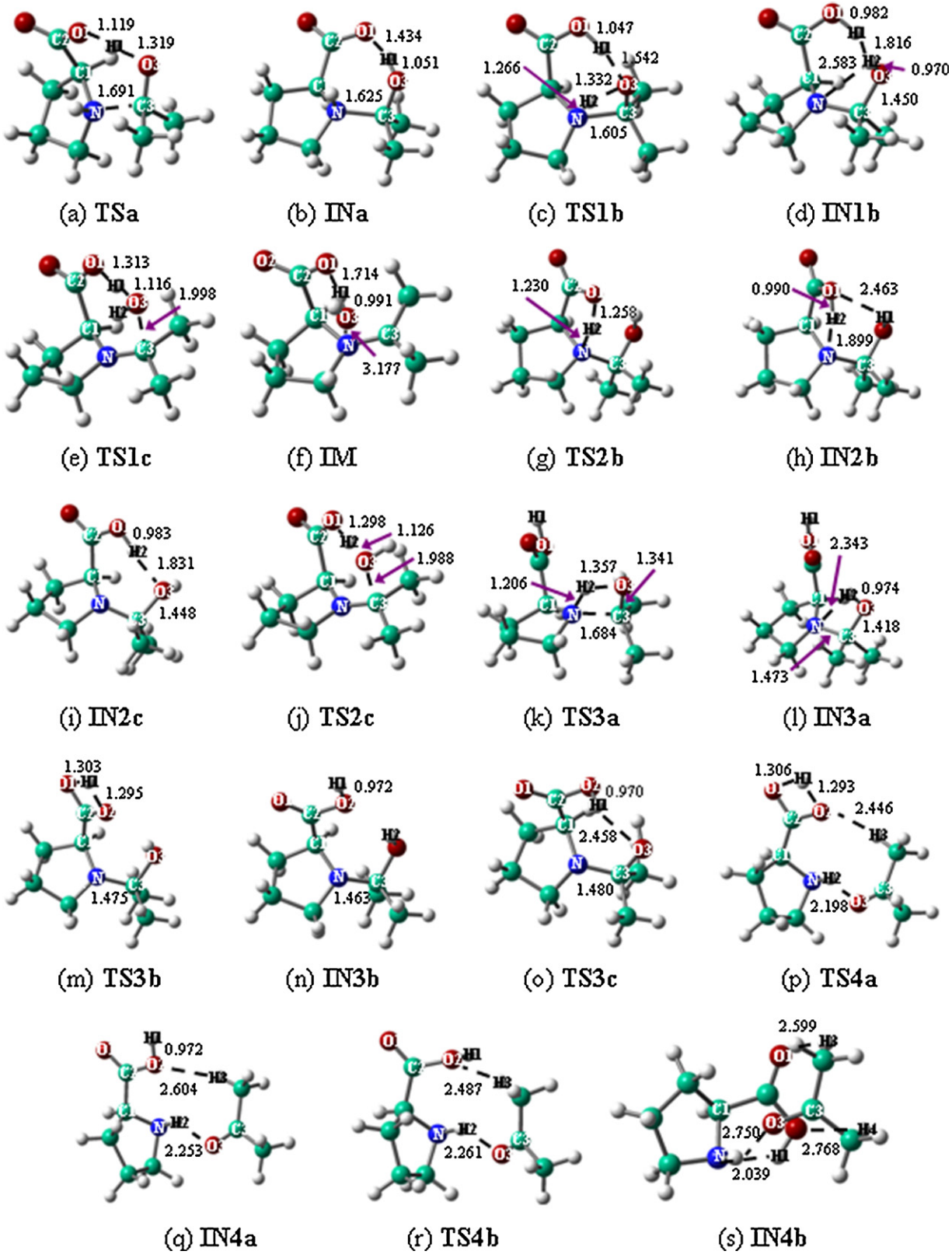

Fig. 3. (a)–(s) Structures of transition states, intermediates and products of the proline-catalyzed aldol reaction.

the lowest energy. Accordingly, **PAa** rather than **PAb** was chosen for the catalysis studies by **Pro1**.

Besides the route of Boyd et al. [24], another two were explored and the energy profiles plotted in Fig. 2. The structures of the transition state (TS) and intermediate (IN) were shown in Fig. 3. In both Routes 1 and 2, Step 1 (**PAa** → **INa**) is the formation of C3–N bond; meanwhile, the carboxyl-H1 atom is spontaneously transferred to bond with the acetone-O3 atom. Owing to the absence of the four-membered ring, the transition state **TSa** is much more stable than the one of Boyd et al. (**1b** in Scheme 1). Accordingly, the energy bar-

rier was lowered to 86 kJ mol^{-1}. The subsequent steps of Routes 1 and 2 differ from each other. As to Route 1, Step 2 (**INa** → **IN1b**) is the transfer of the amino-H2 atom to the carbonyl-O3 atom. It was found the transition state **TS1b** is characterized by a four-membered ring consisting of N, H2, O3 and C3 atoms, similar to **1b** in Scheme 1. However, the energy barrier of this step amounts to 69 kJ mol^{-1} and is much smaller than the value 171 kJ mol^{-1} of the route in Scheme 1. It is due to that the **INa** structure is also unstable in geometry and thus reduces the energy barrier. **TS1b** was calculated 165 kJ mol^{-1} higher in energy than **PAa**, close to the value 171 kJ mol^{-1} of the route in Scheme 1 [24]. Step 3 (**IN1b** → **IM**) is the formation of the imine structure and has a low energy barrier of 37 kJ mol^{-1}. The following steps to form the enamine intermediate are identical to those of Boyd et al. [24] and will not be elaborated here.

As to Route 2, Step 2 (**INa** → **IN2b**) is the intra-proton transfer within the proline fragment, from the amino group to the carboxyl group. It proceeds via a barrierless way and the energy barrier equals −22 kJ mol^{-1}. **IN2b** undergoes the conformational transition to **IN2c** (Fig. 3i). Then the imine structure is formed as a result of Step 3 (**IN2c** → **IM**), with the energy barrier of 36 kJ mol^{-1}.

Compared with the route of Boyd et al. [24], the two ones proposed here have smaller energy barriers and thus are more facile to take place. Especially Route 2 has no unstable transition state structures with four-membered rings. In addition, Step 2 of Route 2 is barrierless and will cause the rapid depletion of **INa**, thus accelerating the rate-determining Step 1. Accordingly, Route 2 should be responsible for the aldol catalysis of the first proline isomer (**Pro1**).

The solvent effects of Route 2 were considered, and it was found that the energy barrier of the rate-determining Step 1 is lowered from 86 to 60 kJ mol^{-1}. It indicated that the aldol reaction will be assisted by solvents, consistent with the results of Boyd et al. and Sunoj et al. [24,37,38].

3.3. *Catalytic reaction routes starting from **Pro2***

The second proline isomer (**Pro2**) has three interaction modes with acetone as well, seeing Fig. 1d–f. **PAe** was chosen to initiate the aldol reaction albeit the lower stability than **PAd**. The acetone molecule in **PAd** is orientated towards the carboxyl group instead of towards the amino group, causing the failure to initiate the reaction. In addition, the high concentration of acetone was used in experiments [1], indicating that it is of high possibility for more than one acetone molecule around proline. It was confirmed by the present density functional calculations. As shown in Fig. 4, the orientations of the two acetone molecules are very close to those in **PAd** and **PAe**, confirming the rationality of choosing **PAe** to initiate the reaction.

Different from **PAa**, the carboxyl-H1 atom in **PAe** is not close to the acetone carbonyl group. If the aldol reaction of **PAe** is started in a similar way as Routes 1 and 2, two negatively charged O atoms (O2 and O3) will approach each other and cause large mutual repulsions. As a result, no geometrically stable intermediates can be located. Accordingly, the formation of C3–N bond as Step 1 (**PAe** → **IN3a**, Route 3 in Fig. 5) has to undergo a transition state with a four-membered ring. The transition state and intermediate structures of Route 3 were shown in Fig. 3. The energy barrier was calculated to be 180 kJ mol^{-1}, which is even slightly larger than that of Boyd et al. [24]. Step 2 (**IN3a** → **IN3b**) is the intra-carboxyl proton transfer within proline. The energy barrier equals 125 kJ mol^{-1}, close to the value 132 kJ mol^{-1} in the case of glycine [39]. Step 3 (**IN3b** → **IN3c**) is the rotation of the O2–H1 bond and needs to cross over a barrier of 51 kJ mol^{-1}. Step 4 (**IN3c** → **IM**) is the same as Step 2 of Route 2, with the energy barrier calculated at 36 kJ mol^{-1}.

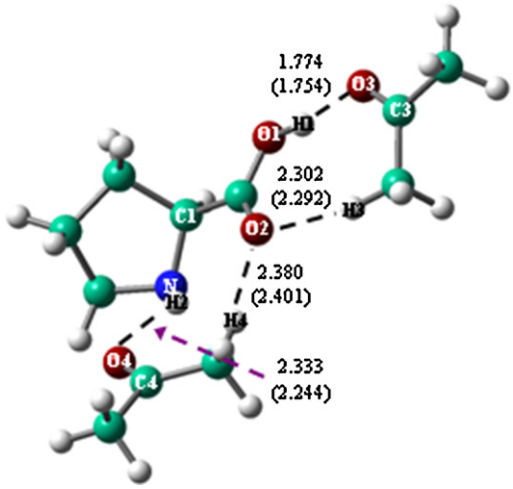

Fig. 4. Structure of proline interacting with 2 mole equiv. acetone. The distances of **PAd** (Fig. 1d) and **PAe** (Fig. 1e) were given in parentheses.

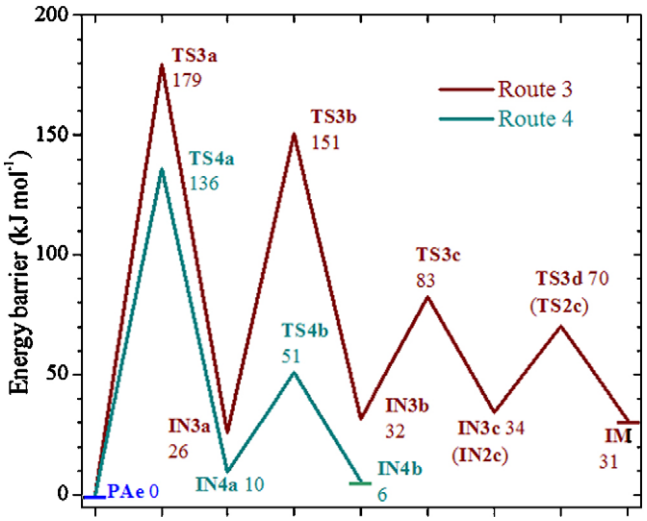

Fig. 5. Energy profiles of the imine formation starting from **PAe**. The structures within and outside the parentheses are the same; that is, **IN3c** and **TS3d** are identical to **IN2c** (Fig. 3i) and **TS2c** (Fig. 3j), respectively.

Owing to the presence of **TS3a** with a four-membered ring, Route 3 is energy-consuming and the aldol reaction is unlikely to proceed via this mechanism. As Route 4 in Fig. 5 indicated, the aldol reaction of **PAe** can also be started with the intra-carboxyl proton transfer process, with the related structures depicted in Fig. 3. The intra-carboxyl proton transfer (**PAe** → **IN4a**) as Step 1 requires an energy of 136 kJ mol^{-1} and is much smaller that of Step 1 in Route 3. Step 2 (**IN4a** → **IN4b**) is the rotation of the carboxyl O2–H1 bond, and the energy barrier amounts to 41 kJ mol^{-1}. **IN4b** (Fig. 3s) geometrically resembles **PAc** (Fig. 1c), which may undergo conformational transition towards **PAa** and continue the aldol reaction. As the previous results suggested, the proton transfer is a solvent-assisted process [24,39–43]. For example, the addition of a water molecule reduces the intra-carboxyl proton transfer of glycine from 132 to 57 kJ mol^{-1} at MP2/6-31G(d,p) level corrected with zero-point vibrational energies (ZPVE) [39].

4. Conclusions

The proline-catalyzed direct aldol reaction is a recent focus and proceeds via an enamine-mediated mechanism. Boyd et al. [24]

proposed a reaction route to form the important enamine intermediate; however, a revisit is absolutely needed due to the lack of conformational search on the interacting modes between proline and acetone as well as the large energy barrier of Step 1 caused by the instability of the first transition state (**1b** in Scheme 1).

Six energy minima were determined for the proline and acetone interacted system. Their relative stabilities increase in the order **PAf** < **PAe** < **PAb** < **PAc** < **PAa** < **PAd** (Fig. 1). All of them are stabilized through the hydrogen bonds of the proline-H atoms and the acetone carbonyl-O atoms as well as the proline carboxyl-O and acetone methyl-H interactions. **PAd** with the proline carboxyl-H atom as the hydrogen bonding donor is the global minimum on the potential energy surface (PES).

As to the first isomer of proline, **PAa** was chosen to initiate the aldol reaction due to its higher stability. Besides the one of Ref. [24], another two reaction routes were explored (Fig. 2). Step 1 with the formation of C3–N bond is rate-determining for both Routes 1 and 2, where the carboxyl-H1 atom is spontaneously transferred to the acetone-O3 atom. Owing to the absence of the four-membered ring in the transition state, the energy barrier was lowered from 171 to 86 kJ mol^{-1}. Route 2 is the most probable to take place because of the barrierless Step 2. In addition, the aldol reaction was found to be assisted by solvents with the reduction of energy barriers.

As to the second isomer of proline, **PAe** was chosen to initiate the aldol reaction. **PAd** has higher stability but fails to initiate the reaction. When 2 mole equiv. acetone was used, the interacting modes of **PAd** and **PAe** co-exist, confirming the initiation by **PAe** since the acetone concentrations are high in experiments. Two reaction routes were obtained (Fig. 5), and the one started with the intra-carboxyl proton transfer is preferred. The energy barrier of Step 1 is rate-determining and equals 136 kJ mol^{-1}; however, it will be greatly assisted by solvents. The subsequent step requires a low energy barrier and reaches an intermediate geometrically resembling **PAc**. Accordingly, it may undergo conformational transition towards **PAa** and continue the aldol reaction until the product formation.

Acknowledgements

We are grateful for the financial supports from the Major State Basic Research Development Program (No. 2004CB719902) and the Talented Funds of Northeast Forestry University (No. 220-602042). We thank the authors of Ref. [24] for offering the Cartesian coordinates of the structures in Scheme 1.

References

[1] B. List, R.A. Lerner, C.F. Barbas III, J. Am. Chem. Soc. 122 (2000) 2395–2396.
[2] B. List, P. Pojarliev, C. Castello, Org. Lett. 3 (2001) 573–575.
[3] K. Sakthivel, W. Notz, T. Bui, C.F. Barbas III, J. Am. Chem. Soc. 123 (2001) 5260–5267.
[4] Z. Tang, F. Jiang, X. Cui, L.Z. Gong, A.Q. Mi, Y.Z. Jiang, Y.D. Wu, Proc. Natl. Acad. Sci. U.S.A. 101 (2004) 5755–5760.
[5] M. Raj, S.K.V. Ginotra, V.K. Singh, Org. Lett. 8 (2006) 4097–4099.
[6] S. Guizzetti, M. Benaglia, L. Pignataro, A. Puglisi, Tetrahedron: Asymmetry 17 (2006) 2754–2760.
[7] D. Enders, T. Gasperi, Chem. Commun. (2007) 88–90.
[8] M. Wiesner, J.D. Revell, H. Wennemers, Angew. Chem. Int. Ed. 47 (2008) 1871–1874.
[9] S. Bahmanyar, K.N. Houk, J. Am. Chem. Soc. 123 (2001) 11273–11283.
[10] L. Hoang, S. Bahmanyar, K.N. Houk, B. List, J. Am. Chem. Soc. 125 (2003) 16–17.
[11] S. Bahmanyar, K.N. Houk, H.J. Martin, B. List, J. Am. Chem. Soc. 125 (2003) 2475–2479.
[12] M. Arno, L.R. Domingo, Theor. Chem. Acc. 108 (2002) 232–239.
[13] C. Allemann, R. Gordillo, F.R. Clemente, P.H. Cheong, K.N. Houk, Acc. Chem. Res. 37 (2004) 558–569.
[14] F.R. Clemente, K.N. Houk, Angew. Chem. Int. Ed. 43 (2004) 5766–5768.
[15] F.R. Clemente, K.N. Houk, J. Am. Chem. Soc. 127 (2005) 11294–11302.
[16] A. Bassan, W.B. Zou, E. Reyes, A. Córdova, Angew. Chem. Int. Ed. 44 (2005) 7028–7032.
[17] C.B. Shinisha, R.B. Sunoj, Org. Biomol. Chem. 5 (2007) 1287–1294.
[18] F.J.S. Duarte, E.J. Cabrita, G. Frenking, A.G. Santos, Eur. J. Org. Chem. 73 (2008) 3397–3402.
[19] G. Angelici, R.J. Corrêa, S.J. Garden, C. Tomasini, Tetrahdron: Asymmetry 50 (2009) 814–817.
[20] M.E. Jung, Tetrahedron 32 (1976) 3–31.
[21] K.L. Brown, L. Damm, J.D. Dunitz, A. Eschenmoser, R. Hobi, C. Kratky, Helv. Chim. Acta 61 (1978) 3108–3135.
[22] C. Puchot, O. Samuel, E. Dunach, S. Zhao, C. Agami, H.B. Kagan, J. Am. Chem. Soc. 108 (1986) 2353–2357.
[23] B. List, L. Hoang, H.J. Martin, Proc. Natl. Acad. Sci. U.S.A. 101 (2004) 5839–5842.
[24] K.N. Rankin, J.W. Gauld, R.J. Boyd, J. Phys. Chem. A 106 (2002) 5155–5159.
[25] A.M. Sapse, L.M. Levy, S.B. Daniels, B.W. Erickson, J. Am. Chem. Soc. 109 (1987) 3526–3529.
[26] S.G. Stepanian, I.D. Reva, E.D. Radchenko, L. Adamowicz, J. Phys. Chem. A 105 (2001) 10072–10664.
[27] E. Czinki, A.G. Császár, Chem. Eur. J. 9 (2003) 1008–1019.
[28] W.D. Allen, E. Czinki, A.G. Császár, Chem. Eur. J. 10 (2004) 4512–4517.
[29] S.X. Tian, J.L. Yang, Angew. Chem. Int. Ed. 45 (2006) 2069–2072.
[30] M.J. Frisch, G.W. Trucks, H.B. Schlegel, G.E. Scuseria, M.A. Robb, J.R. Cheeseman, J.A. Montgomery, T. Vreven Jr., K.N. Kudin, J.C. Burant, J.M. Millam, S.S. Iyengar, J. Tomasi, V. Barone, B. Mennucci, M. Cossi, G. Scalmani, N. Rega, G.A. Petersson, H. Nakatsuji, M. Hada, M. Ehara, K. Toyota, R. Fukuda, J. Hasegawa, M. Ishida, T. Nakajima, Y. Honda, O. Kitao, H. Nakai, M. Klene, X. Li, J.E. Knox, H.P. Hratchian, J.B. Cross, C. Adamo, J. Jaramillo, R. Gomperts, R.E. Stratmann, O. Yazyev, A.J. Austin, R. Cammi, C. Pomelli, J.W. Ochterski, P.Y. Ayala, K. Morokuma, G.A. Voth, P. Salvador, J.J. Dannenberg, V.G. Zakrzewski, S. Dapprich, A.D. Daniels, M.C. Strain, O. Farkas, D.K. Malick, A.D. Rabuck, K. Raghavachari, J.B. Foresman, J.V. Ortiz, Q. Cui, A.G. Baboul, S. Clifford, J. Cioslowski, B.B. Stefanov, G. Liu, A. Liashenko, P. Piskorz, I. Komaromi, R.L. Martin, D.J. Fox, T. Keith, M.A. Al-Laham, C.Y. Peng, A. Nanayakkara, M. Challacombe, M.W.P. Gill, B. Johnson, W. Chen, M.W. Wong, C. Gonzalez, J.A. Pople, Gaussian 03. Revision D. 01, Gaussian, Inc, Wallingford, CT, 2004.
[31] A.D. Becke, J. Chem. Phys. 88 (1988) 2547–2551.
[32] C. Lee, W. Yang, R.G. Parr, Phys. Rev. B 37 (1988) 785–789.
[33] S. Mietus, E. Scrocco, J. Tomasi, J. Chem. Phys. 55 (1981) 117–122.
[34] G. Yang, X.W. Han, W.P. Zhang, X.M. Liu, P.Y. Yang, Y.G. Zhou, X.H. Bao, J. Phys. Chem. B 109 (2005) 18690–18698.
[35] G. Yang, Y.G. Zu, C.B. Liu, Y.J. Fu, L.J. Zhou, J. Phys. Chem. B 112 (2008) 7104–7110.
[36] Z.W. Yang, G. Yang, Y.G. Zu, Y.J. Fu, L.J. Zhou, Phys. Chem. Chem. Phys. (2009), doi:10.1039/B909299D.
[37] S. Kotha, S. Banerjee, M.P. Patil, R.B. Sunoj, Org. Biomol. Chem. 4 (2006) 1854–1856.
[38] M.P. Patil, R.B. Sunoj, Chem. Asian J. 4 (2009) 714–724.
[39] G. Yang, X.M. Wu, Y.G. Zu, C.B. Liu, Y.J. Fu, L.J. Zhou, Int. J. Quantum Chem. 109 (2009) 320–327.
[40] G.A. Voth, Acc. Chem. Res. 39 (2006) 143–150.
[41] X.C. Wang, J. Nichols, M. Feyereisen, M. Gutowski, J. Boatz, A.D.J. Haymet, J. Simons, J. Phys. Chem. 95 (1991) 10419–10425.
[42] Q. Zhang, R. Bell, T.N. Truong, J. Phys. Chem. 99 (1995) 592–599.
[43] B. Balta, V. Aviyente, J. Comput. Chem. 25 (2004) 690–703.